

# Mapping Functional Connectivity Using Potts Spin Model

L. I. Stanberry<sup>1</sup>, A. Murua<sup>2</sup>, D. Cordes<sup>3</sup>

<sup>1</sup>Statistics, University of Washington, Everett, WA, United States, <sup>2</sup>Mathematics, University of Montreal, Montreal, QC, Canada, <sup>3</sup>Radiology, University of Washington, Seattle, WA, United States

**Introduction** fMRI studies with complex activation paradigms or unknown brain response patterns (e.g. drug studies, epileptic seizures or resting-state data) can be analyzed by clustering methods. Even though these techniques are regarded as exploratory and data-driven, the cluster identification depends on the number of expected clusters or the value of the chosen threshold, the details which are not known a priori. Here we present a clustering method based on the Potts spin model which makes no assumption of the distribution of the data. The number of distinct groups in the data is determined as the number of connected components at the temperature where the jump of the average variance associated with the largest cluster sizes occurs. This method was originally reported by Blatt et al [1] and extended by Murua et al. [2].

**Theory** A q-state Potts spin model assumes a lattice composed of spins in q-possible orientations (a model with two spin orientations is an Ising model). If the configuration of the system, defined by the interaction energy of the pairs of spins, is such that spins of the same orientation have higher interaction energy than spins of different orientations, then the lattice splits into homogenous domains each containing only spins of the same orientation. This partition is equivalent to the clustering of data into distinct groups, or *clusters*, which contain objects with similar characteristics. In a data set consisting of N-points (voxels)  $v_1, \dots, v_N$ , the interaction,  $J_{ij}$ , between voxels  $v_i$  and  $v_j$  is defined as an increasing function of the correlation coefficient. The data now can be viewed as a weighted graph with weights determined by the pairwise interactions. If  $S = \{s_1, \dots, s_N\}$  is the cluster membership of the data points, then the probability density of the cluster assignment,  $S$ , at temperature,  $T$ , is given by the Boltzmann distribution:

$$P(S) = \exp\left(-\frac{H(S)}{T}\right) / \sum_S \exp\left(-\frac{H(S)}{T}\right) \text{ where the Hamiltonian, } H(S), \text{ specifies the energy of the given system: } H(S) = \sum_{(i,j)} J_{ij}(1 - \delta_{s_i s_j})$$

where  $\delta_{ij}$  is a Kronecker delta and the summation is defined over all *neighboring* sites  $v_i$  and  $v_j$ . In large data sets the construction of a complete graph is computationally expensive. One might instead define, for example, a  $K$ -nearest neighbor (Knn) graph where voxels  $v_i$  and  $v_j$  are said to be neighbors if and only if  $v_j$  is among  $K$ -nearest neighbors of  $v_i$ , and  $v_i$  is among  $K$ -nearest neighbors of  $v_j$ . The size of the neighborhood,  $K$ , could be chosen to produce a connected graph. However, if the size of the neighborhood,  $K$ , which allows for feasible computations, produces a graph with multiple connected components, then the  $Knn$ -graph can be augmented by edges of the minimum-spanning tree. To determine the underlying structure of the data one needs to find a group assignment,  $S$ , which has a high probability at temperature,  $T$ . This is done using an augmented variable Markov Chain Monte Carlo technique as follows. Consider a Bernoulli variable  $b_{ij}$  which may take the value one ("frozen" bond) whenever voxels  $v_i$  and  $v_j$  are neighbors and belong to the same cluster, and zero otherwise (not frozen bond). The joint density of bonds,  $B$ , and cluster assignments,  $S$ , can be written as

$$p(S, B) = Z^{-1} \prod_{(i,j)} ((1 - p_{ij})(1 - b_{ij}) + p_{ij} b_{ij} \delta_{s_i s_j})$$

where  $p_{ij} = 1 - \exp(-J_{ij}/T)$  is the probability of the bond to be frozen. To generate samples from the Potts model, a Gibbs sampler starts with random assignments of spins to the clusters (e.g. all spins could be assigned to the same cluster) and proceeds by alternating between the two steps: (a) Given the cluster configuration,  $S$ , determine bond,  $b_{ij}$ , to be frozen with probability as specified by previous formula if two points are neighbors and belong to the same cluster; else set  $b_{ij}$  to zero. (b) Given the bond configuration,  $B$ , assign the connected subset – a set of points connected by the frozen bonds – to the same cluster. At any given temperature  $M$ -simulated samples are collected giving rise to  $M$  possible system configurations  $S_1, \dots, S_M$ . The probability of two voxels being at the same cluster is

estimated as  $\hat{\delta}_{ij} = \sum_{S_k, k=1:M} \delta_{ij}^{S_k} / M$ , where  $\delta_{ij}^{S_k}$  is an indicator of two voxels belonging to the same cluster under system configuration  $S_k$ . Two voxels are

assigned to the same cluster if the estimated probability exceeds the specified threshold. The resulting assignment is specific to the given temperature,  $T$ . In general following the Potts spin model we would expect to observe three distinct phases for the system with the underlying group structure: (1) low temperature phase when all the points form a single cluster; (2) intermediate phase, where strongly coupled interactions are present, but weak interactions are already dissolved by the rising temperature; (3) high temperature phase, where both strong and weak interactions vanished resulting in multiple clusters of small sizes. To determine the range of temperatures defining a stable phase of the system one could monitor the variance of the size of the largest clusters for various temperatures. We used an Adjusted Rand index (ARI) to compare the agreement between the cluster assignments at neighboring temperatures. The higher the value of the ARI the more alike two partitions are.

**Methods** fMRI was performed using a commercial 1.5T GE MRI scanner with parameters: TR 0.4s, Flip 50, 4 axial slices, FOV 24x24, BW +/- 62.5 KHz, thick 7mm/2mm, 64x64, 750 time points. Potts model clustering was applied to the data from the motor task (30 identical cycles of finger tapping and rest with a 10s period). The time series were normalized to have mean zero and standard deviation one. To reduce the size of the data set only voxels having low-frequency (~0.02-0.12Hz) specific correlations of at least 0.3 with five or more voxels were retained. The burn in size was set to 500 sweeps and the following 500 sweeps were used to determine cluster assignments.

**Results and Conclusion** Peaks of the variance curves (Fig.1, left) indicate the critical temperatures associated with significant changes in cluster structures. Voxels comprise a unique cluster at the initial low temperatures (Fig.1, center), but once the log- $T$  exceeds -1.61 (Fig.1, left, 1<sup>st</sup> peak) the single cluster splits into 4 distinct clusters. The system remains in this state until the next transition occurs at log- $T$  of -0.92 (Fig.1, left, 2<sup>nd</sup> peak). The ARI (Fig.1, right) is one until the first critical temperature is attained. During the 2<sup>nd</sup> phase ARI is ~0.8. Once the log- $T$  exceeds -0.92 the agreement between the cluster assignments at neighboring temperatures drops below 0.4. The clustering results at -0.92 (Fig.2) show the large red cluster which corresponds to the motor cortex and SMA. The remaining clusters represent motion component and vascular contributions. Frequency spectra and wavelet power spectra (Fig.3) show a strong contribution from the paradigm frequency (0.1Hz) to the time courses of all, but the 3<sup>rd</sup>, clusters. The power of the task frequency closely mimics the task design in the motor areas. Respiratory artifacts are noticeable in the second largest cluster as the periodic spikes at around 0.4Hz. The clustering at slightly higher log-temperature of -0.86 (Fig.4) shows that the disordered system as the red cluster associated with the motor task splits into various small cluster groups.

**References** [1] Blatt et al (1997) Neural Computation 9, 1805-1842. [2] Murua et.al. Technical Report, University of Washington

Figure 1

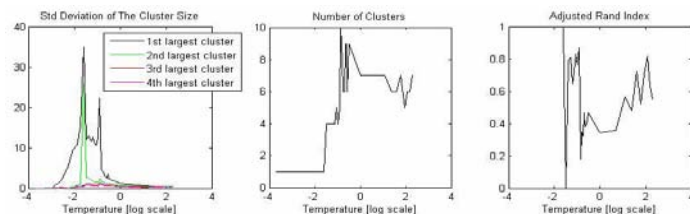


Figure 2(right)  
Figure 4(below)

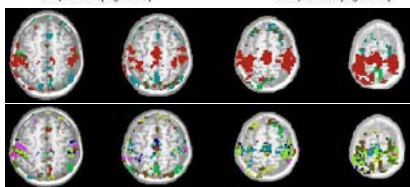


Figure 3

